Journal of Peptide Science
J. Pept. Sci. 2008; **14**: 66–75
Published online 11 October 2007 in Wiley InterScience (www.interscience.wiley.com). DOI: 10.1002/psc.913

JOURNAL OF PEPTIDE SCIENCE

Self-assembly of the octapeptide lanreotide and lanreotide-based derivatives: the role of the aromatic residues

ANJALI PANDIT,[a,d] NICOLAS FAY,[a] LUC BORDES,[a] CÉLINE VALÉRY,[b] ROLAND CHERIF-CHEIKH,[b] BRUNO ROBERT,[a] FRANCK ARTZNER[c] and MAÏTÉ PATERNOSTRE[a]*

[a] IBITECS, CEA and CNRS, F-91191 Gif-sur-Yvette, France
[b] Ipsen/Pharma, Barcelona, Spain
[c] GMCM, UMR 6626, 35042 Rennes, France
[d] Leiden Institute of Chemistry, Gorlaeus Laboratories Leiden University, PO Box 9502 2300 RA Leiden, The Netherlands

Received 5 April 2007; Revised 28 June 2007; Accepted 6 July 2007

Abstract: We investigated the spectroscopic properties of the aromatic residues in a set of octapeptides with various self-assembly properties. These octapeptides are based on lanreotide, a cyclic peptide analogue of somatostatin-14 that spontaneously self-assembles into very long and monodisperse hollow nanotubes. A previous study on these lanreotide-based derivatives has shown that the disulfide bridge, the peptide hairpin conformation and the aromatic residues are involved in the self-assembly process and that modification of these properties either decreases the self-assembly propensity or modifies the molecular packing resulting in different self-assembled architectures. In this study we probed the local environment of the aromatic residues, naphthyl-alanine, tryptophan and tyrosine, by Raman and fluorescence spectroscopy, comparing nonassembled peptides at low concentrations with the self-assembled ones at high concentrations. As expected, the spectroscopic characteristics of the aromatic residues were found to be sensitive to the peptide–peptide interactions. Among the most remarkable features we could record a very unusual Raman spectrum for the tyrosine of lanreotide in relation to its propensity to form H-bonds within the assemblies. In Lanreotide nanotubes, and also in the supramolecular architectures formed by its derivatives, the tryptophan side chain is water-exposed. Finally, the low fluorescence polarization of the peptide aggregates suggests that fluorescence energy transfer occurs within the nanotubes. Copyright © 2007 European Peptide Society and John Wiley & Sons, Ltd.

Supplementary electronic material for this paper is available in Wiley InterScience at http://www.interscience.wiley.com/jpages/1075-2617/suppmat/

Keywords: self-assembly process; peptide nanotubes; aromatic interactions; fluorescence spectroscopy; Raman spectroscopy

INTRODUCTION

The ability of small molecules to spontaneously organize themselves into well-defined structures underlies the variety of self-assembled bio-structures found in nature and a wide-range of applications in nanotechnology [1,2]. The key elements for assembly of natural or biomimetic structures are the noncovalent interactions between the self-organizing molecules, that is hydrogen and ionic bonds, hydrophobic effect and van der Waals interactions [3,4]. These elements determine the shapes of biological supramolecular structures such as tubuli and filaments. The emergence of amyloid related diseases increases the interest of the scientific community in studying the key motifs for protein folding, self-assembly mechanisms, molecular structures and kinetic pathways for formation [5–12]. Studies on small synthetic peptides have provided insight into the specific interacting forces that govern self-assembly into fiber-like structures [13–16]. Moreover, the tunable chemical structures of novel peptides and hybrid peptide amphiphile molecules allow the control of the self-assembly process resulting in different supramolecular architectures and leading to the design of new materials [17–21].

We recently discovered that a set of small peptides have exceptional self-organizing properties [22,23]. These analogues are based on the synthetic octapeptide lanreotide (NH_3-(D)Naph-Cys-Tyr-(D)Trp-Lys-Val-Cys-Thr-$CONH_2$): a growth hormone inhibitor that is in use as a pharmaceutical treatment of agromegaly, a hormonal disorder that results when excess growth hormone is produced by the pituitary gland. In the concentration range of 3–18% (w/w) lanreotide in water forms a gel that consists of unique structures: hollow nanotubes with diameters of 24 nm and lengths up to hundreds of micrometers. The nanotube walls are built up from helicoidal filaments, formed by peptide dimer building blocks self-assembled into antiparallel β-sheets through an alternating pattern of the aliphatic and aromatic aminoacid residues [22]. The temperature/concentration phase diagram of lanreotide in

*Correspondence to: M. Paternostre, IBITECS, SB^{2}SM, URA CNRS 2096, Batiment 532, Cea-Saclay, 91191 Gif-sur-Yvette, France;
e-mail: maite.paternostre@cea.fr

water was studied and showed different structural phases [23]. Depending on the concentration, the lanreotide self-assembles either in monodisperse or in polydisperse and embedded nanotubes. The molecular packing inside the nanotube walls strongly supports the idea that aromatic side chains are involved in the self-assembly process, and we recently demonstrated this involvement by a mutational approach [24]. Besides the participation of these aromatic side chains, we have also demonstrated that the amphiphilicity of the molecule drives its molecular packing inside the supramolecular architectures and also drives the morphology of the final objects. The upper picture in Figure 1 summarizes the supramolecular structures formed by lanreotide and six lanreotide analogues. The lower picture is deduced from [22] and presents the molecular packing of lanreotide inside the nanotubes.

To summarize, the sequence of lanreotide contains a set of key elements that drive self-association with a high degree of hierarchical ordering and allow tuning of its supramolecular structures by selective modification. Lanreotide self-assembles through the formation of β-sheet networks, giving to the nanotubes an amyloid-like character. The word 'amyloid', meaning 'starch-like', was given by mistake to extracellular protein aggregates found in the organs of patients suffering from amylose, because these aggregates were stained by iodine like starch [25]. Later, it was discovered that amyloids were in fact protein precipitates constituted by ordered fiber/filament structures, which were stabilized by extended intermolecular β-sheet [26]. Therefore, we use the term 'amyloid' to qualify fibers, filaments and even nanotube structures when they involve an extended intermolecular β-sheet network. The techniques used to reveal the amyloid character of protein/peptides aggregates are multiple, either based on undirected observation, i.e. using external probes (Congo-red or Thioflavine T [9,27] that interact with the amyloid fibers, or on direct visualization using electron microscopy [28] and more recently AFM [29,30]. Concerning the indirect methods using dyes to reveal the amyloid nature of the fibrils, the dye to fibril interaction mechanisms are still under debate [31] and in some cases can interact with the fibril growth mechanisms as shown by [32]. For the lanreotide and derivative assemblies, we chose other methods such as IR spectroscopy and X-ray scattering to characterize the β-sheet network content of our amyloid type architectures. These approaches that have been widely used in the past to reveal the amyloid character of fibers, give in our case, due to the size and simplicity of the molecule, precise and quantitative information [22,23].

The loss of supramolecular structures upon selective modification of tyrosine or naphthylalanine into phenylalanine indicates that hydrogen bonding and π-stacking are involved in the very first steps of the self-assembly process. In addition, modification of the amphiphilicity of the peptide by substituting the lysine with a D-lysine changes the molecular packing of the peptide and in turn also tunes the final supramolecular architectures from nanotubes to amyloid fibres. Therefore lanreotide and lanreotide-based derivatives could be interesting model systems for the study of protein fibril formation.

In this work, a combination of electronic and vibrational spectroscopies is applied to probe the local environment of the aromatic amino acid residues in lanreotide and a set of lanreotide derivatives. In the latter, chemical groups have selectively been modified as summarized in Figure 1, and their behavior in water has been studied. Here we aim to explore the use of fluorescence and Raman spectroscopy to compare the aromatic intermolecular interactions that occur in these assemblies. The set of selectively-modified derivatives allows us to assign the individual Raman bands. Our peptides on one hand are simple and well-defined systems compared to large proteins, but on the other hand contain all the properties of aromatic side chains in a protein environment. In this context, our study is complementary to Raman studies on aromatic molecules in various solvents that are used as model systems for the behavior of aromatic residues in proteins.

EXPERIMENTAL

Peptide Sequences

(**1**) Lanreotide NH_3-(D)Naph-cyclo-[Cys-Tyr-(D)Trp-Lys-Val-Cys]-Thr-$CONH_2$ (**2**) DTrp → DPhe NH_3-(D)Naph-cyclo-[Cys-Tyr-(D)Phe-Lys-Val-Cys]-Thr-$CONH_2$ (**3**) DNaph → DPhe NH_3-(D)Phe-cyclo-[Cys-Tyr-(D)Trp-Lys-Val-Cys]-Thr-$CONH_2$
(**4**) DNaph → DAla NH_3-(D)Ala-cyclo-[Cys-Tyr-(D)Trp-Lys-Val-Cys]-Thr-$CONH_2$ (**5**) Tyr → Phe NH_3-(D)Naph-cyclo-[Cys-Phe-(D)Trp-Lys-Val-Cys]-Thr-CO NH_2 (**6**) Cys → Ala NH_3-(D)Naph-Ala-Tyr-(D)Trp-Lys-Val-Ala-Thr-$CONH_2$ (**7**) Lys → DLys NH_3-(D)Naph-cyclo-[Cys-Tyr-(D)Trp-(D)Lys-Val-Cys]-Thr-$CONH_2$

Materials and sample preparation. Lanreotide and the derivative acetate powder were obtained from Ipsen Pharma (Barcelona, Spain) under the reference H008/2 100 006 and K008/2 100 006. The peptides were synthesized by a Kinerton batch process (Dublin, Ireland), which includes a flash-freeze lyophilization. The peptide solutions were prepared by adding deionized water to a weighted fraction of peptide acetate powder. The samples were prepared at least 24 h before the experiments and stored at 4 °C. For measurements on naphthalene Raman spectra in organic solvents, the organic solvents were freshly distilled and kept on molecular sieves that had been activated in an oven at 500 °C for 48 h. The organic solvent was kept in a dry hood and used within 2 days. Ether and tetrahydrofuran (THF) were distilled from sodium/benzophenone and dichloromethane (CH_2Cl_2) was distilled from CaH_2. Methanol was dried by standing with 4 Å molecular sieves.

Fluorescence spectroscopy. Fluorescence spectra were measured on a Spex Fluorolog 0.34 M spectrophotometer,

DOI: 10.1002/psc

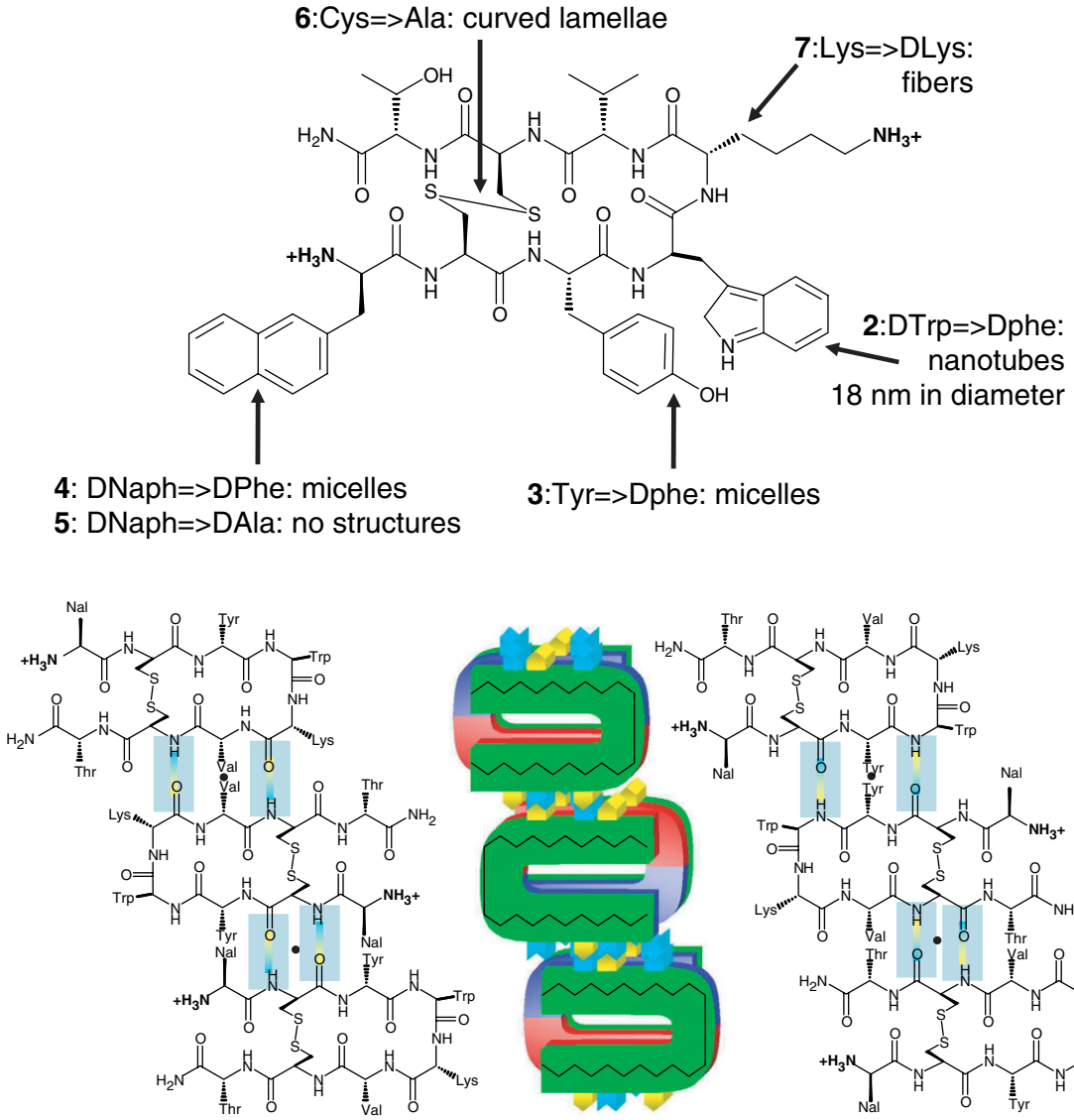

Figure 1 (a) Chemical structure of lanreotide (**1**) and the effects of aminoacid substitutions DTrp => DPhe (**2**), Tyr => Phe (**3**), DNaph=>DPhe (**4**), DNaph=>DAla (**5**), Cys=>Ala (**6**) and Lys=>DLys (**7**) on the self-assemblies. (b) Packing model for lanreotide nanotubes, adapted from Valery C, *et al.* Biomimetic organization: Octapeptide self-assembly into nanotubes of viral capsid-like dimension. *Proc. Natl. Acad. Sci. U.S.A.* 2003; **100**(18): 10 258–10 262 (Copyright (2007) National Academy of Sciences, U.S.A.). The nanotube walls are built up from two types of curled filaments. Intermolecular interactions within the β-sheet filaments involve Tyr–Tyr and Thr–Val interactions (type 1 filament, left) and Val–Val interactions (type 2 filament, right).

equipped with a set of Glan–Thompson polarizers. Excitation and fluorescence spectra were collected using slit widths of 2 nm. To reduce scatter artifacts and to gain signal in fluorescence polarization measurements a 280-nm filter was used instead of a slit for excitation and the emission slit width was changed to 10 nm. To remove the Raman scatter, spectra of distilled water were taken under the same conditions and subtracted. Samples were measured in quartz cuvettes and for peptide concentrations exceeding 10^{-3} % w/w they were measured front-face to avoid inner filter effects.

Raman spectroscopy. Two different Raman spectroscopy approaches were used in this work: Raman spectroscopy under pre-resonance conditions, using a 457.9-nm excitation source and FT-Raman spectroscopy using a 1064-nm excitation source. For all the spectra obtained from peptide samples, we needed to use pre-resonance conditions to increase the signal to noise ratio, especially for the lowest peptide concentration. Unfortunately, we could not use real resonance conditions because of the intrinsic fluorescence of the peptide. Fourier transformed Raman spectroscopy, which requires high sample concentrations, was only used on naphthalene in solvents of different polarity, as we were not limited by the concentration. A 457.9-nm excitation source was produced using a tunable Coherent Argon laser (Innova 100 ~ 60 mW output). Spectra were collected by a Jobin-Yvon U1000 Raman spectrophotometer equipped with a liquid nitrogen-cooled CCD detector (Spectrum One, Jobin-Yvon, France) using a CCD detection window of 1800 × 100 and slit widths of 0.25 mm. The resolution under these conditions was 2 cm^{-1}. Data were collected averaging 2–200 measurements of 10 s sampling

DOI: 10.1002/psc

time (per window). Samples were measured using a quartz absorption cuvette oriented front-face. The resulting spectra were analyzed using Datamax for manual background subtraction.

Fourier-transformed Raman spectra were recorded at 4 cm^{-1} resolution using a Bruker IFS66 interferometer coupled to a Bruker FRA106 Raman module equipped with a continuous Nd : Yag laser providing excitation at 1064 nm as described in Mattioli *et al.* [33]. All spectra were recorded at room temperature with backscattering geometry from samples in hermetically closed cuvettes. The spectra resulted from 500 to 5000 coadded interferograms depending on the sample signal.

RESULTS AND DISCUSSION

Fluorescence Spectra of Soluble Peptides and Nanostructures

Both the fluorescence behavior of peptide solutions and the peptide gels containing nanostructure assemblies were characterized. In the solutions, the peptides may exist as monomers or small aggregates (dimers) and this state will further be referred to as the 'soluble peptide' state. Figure 2(a) shows the normalized fluorescence spectra of lanreotide, DTrp-DPhe, DNaph-DPhe, DNaph-DAla, Tyr-Phe and Lys-DLys at peptide solutions at low concentrations (10^{-3} % w/w). The fluorescence of the Cys-Ala peptide will be discussed in a subsequent paper. Although tryptophan and naphthalene have similar extinction coefficients at 280 nm, the only peptide that displays naphthalene fluorescence is the DTrp-DPhe (**2**) and for this peptide the fluorescence quantum yield is very low ($Q = 0.015$, measured using L-tryptophan in water as a reference). Lanreotide, DNaph-DPhe, DNaph-DAla, Tyr-Phe and Lys-DLys (**1, 3–5** and **7**) have typical tryptophan fluorescence spectra. This suggests that in the six soluble peptides the fluorescence of naphthalene is severely quenched by intramolecular interactions. The tryptophan fluorescence maxima of lanreotide, DNaph-DPhe, DNaph-DAla and Tyr-Phe are around 342 nm and the maximum of Lys-DLys is at 345 nm. The fluorescence maxima corresponded to a hydrophilic environment where the tryptophan indole sidechains are water-exposed.

Lanreotide (**1**), DTrp-DPhe (**2**), Cys-Ala (**6**) and Lys-DLys (**7**) are capable of forming nanostructure self-assemblies at high concentrations (>2% w/w) as summarized in Figure 1: lanreotide and DTrp-DPhe assemble into long, hollow, nanotubes, the Cys-Ala forms curved, lamellar sheets and the Lys-DLys assembles into amyloid-like fibers. Macroscopically, concentrated samples of these peptides form stable gels that exhibit birefringence [24]. Figure 2(b) shows the normalized fluorescence spectra of lanreotide, DTrp-DPhe and Lys-DLys at aggregate concentrations, i.e. at 5% w/w (Lys-DLys) or 10% w/w

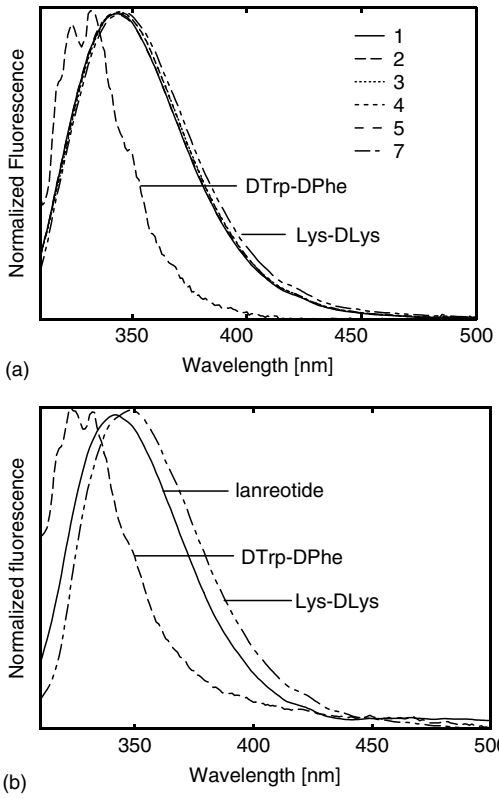

Figure 2 (a) Normailzed fluorescence spectra of the peptides in soluble form; lanreotide (**1**), DTrp-DPhe (**2**), DNaph-DPhe (**3**), DNaph-DAla (**4**), Tyr-Phe (**5**) and Lys-DLys (**7**) (concentration 0.001% w/w). (b) Normalized fluorescence spectra of lanreotide, DTrp-DPhe and Lys-DLys at aggregate concentrations (10% for lanreotide and DTrp-DPhe and 5% w/w for Lys-DLys). Excitation at 275 nm.

(lanreotide and DTrp-DPhe). The fluorescence maximum of the lanreotide nanotube sample is not significantly shifted compared to the soluble peptide spectrum (342 nm compared to 343 nm for the solution) and also the two fluorescence peaks of the DTrp-DPhe spectrum remain at the same values, but with a different intensity ratio. In contrast, the fluorescence maximum of the Lys-DLys fibers is reshifted compared to the fluorescence of the soluble peptides (345 = >348 nm). Also, here the fluorescence maxima correspond to a hydrophilic environment, implying that although incorporated in the self-assemblies, the tryptophan sidechains remain water-exposed.

A striking result is the low Trp fluorescence polarization of lanreotide nanotubes and Lys-DLys fibers ($r = 0.02$ for lanreotide and $r = 0.006$ for Lys-DLys, see Table 1). In contrast, a sample of lanreotide peptides in solution (5×10^{-4}% w/w) dissolved in 99% glycerol has an anisotropy of 0.12. The higher polarization value of lanreotide peptides dissolved in glycerol demonstrates that internal conversion between the L_a–L_b states or interactions within the soluble peptide forms cannot

DOI: 10.1002/psc

Table 1 Tryptophan fluorescence anisotropy values for peptide self-assemblies[a]

peptide	*r*
1 (lanreotide)	0.02
1 (lanreotide) in 99% glycerol	0.12
2 (DTrp-DPhe derivative)	0.15
7 (Lys-DLys derivative)	0.006

[a] for lanreotide in 99% glycerol the concentration was 5×10^{-4}% w/w, for lanreotide and DTrp-DPhe the peptide concentrations were 10% w/w and for Lys-DLys the peptide concentration was 5% w/w.

explain the observed depolarization in the nanostructure aggregates. Also, complete depolarization due to rotational diffusion of the Trp side chain can be ruled out: ultrafast polarized fluorescence studies on single Trp-containing peptides have shown that depolarization through rotational diffusion of the Trp side chains occurs on a time scale of ~50 ps [34,35], after which the remaining anisotropy is still as high as 0.17 (i.e. its rotational freedom is restricted by the peptide backbone). The origin of the fluorescence depolarization is therefore sought to involve intermolecular interactions of tryptophan with aromatic residues. Trp-Trp, Tyr-Trp and Naph-Trp interactions could induce fluorescence energy transfer leading to depolarized tryptophan fluorescence. However, the latter two interactions (Tyr-Trp and Naph-Trp) would still leave a considerable fraction of polarized fluorescence from directly excited tryptophan. Thereby Trp-Trp fluorescence homotransfer is more likely. This effect has been observed in several proteins [36]. Furthermore, Kayser *et al.* showed evidence for Trp-Trp fluorescence energy migration along self-assembled β-sheet ribbons, explaining the low anisotropy value for these self-assemblies [37]. Nanostructure self-assemblies of the DTrp-DPhe peptide, which displays naphthalene fluorescence, have a higher anisotropy ($r = 0.15$) that is of the order expected for large aggregates that have slow rotational diffusion. We did not observe a naphthalene excimer band, which would have been indicative of Naph-Naph intermolecular interactions.

Raman Spectroscopy

To obtain further information on the environment and interactions of the aromatic aminoacid residues, Raman spectroscopy measurements were applied for the set of peptides at two concentrations: 1% w/w, at which the peptides exist in a soluble form and 10% w/w (lanreotide, DTrp-DPhe, DNaph-DPhe, DNaph-DAla, Tyr-Phe, **1-5**) or 5% w/w (Cys-Ala and Lys-DLys, **6** and **7**), at which concentrations the lanreotide, DTrp-DPhe, Cys-Ala and Lys-DLys peptides form ordered nanostructures as described above. By comparing the Raman spectra of the derivatives that alternatively lack one of the aromatic residues, the bands of naphthylalanine, tyrosine and tryptophan can easily be assigned. The results for each aromatic residue are presented below.

Naphthylalanine. In the series of spectra shown in Figure 3, lanreotide, the tryptophan-modified derivative DTrp-DPhe (**2**) and the cysteine modified derivative Cys-Ala **6**) the spectra show a significant (3–5 wavenumbers) downshift of the naphthalene ring frequencies with concentration, i.e. upon self-assembly, whereas for the Tyr (**5**) and the Lys (**7**) modified derivatives the naphthalene band does not change with the concentration.

To test whether the observed downshift could reflect a transition towards a more hydrophobic environment, FT-Raman spectra were recorded of naphthalene powder dissolved in organic solvents (see Supporting information). The results show, however, that the naphthalene Raman frequency modes are insensitive to the polarity of the environment and thus the observed frequency downshift cannot be explained by a transition to a hydrophobic environment upon self-assembly. Assuming that at 1% w/w the peptides are soluble

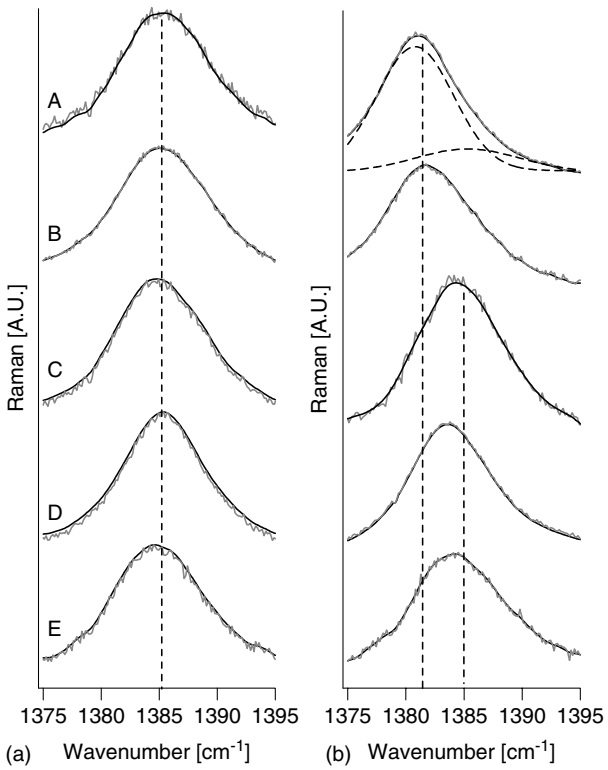

Figure 3 Naphthalene Raman frequency mode of: (A) **1** lanreotide (B) **2** DTrp-DPhe, (C) **5** Tyr-Phe, (D) **6** Cys-Ala and (E) **7** Lys-DLys. (a) concentrations 1% w/w. (b) concentrations 10% w/w (A–C) or 5% w/w (D), (E). For clarity, smoothed spectra (black lines) are plotted on the raw data. For lanreotide (A), also the fitted Raman bands of pure aggregates and soluble peptides are drawn (dashed spectra) that superposed form the 10% spectrum.

DOI: 10.1002/psc

and that at 10% w/w they form equilibria between the soluble form and aggregates, the fraction of soluble form in 10% samples of lanreotide (**1**) and DTrp-DPhe (**2**) and in the 5% w/w sample of Cys-Ala (**6**) can be estimated from the skewness of the Raman bands in Figure 3. For 1% samples, the bands are symmetrical, whereas for 10 and 5% samples they are skewed with a high-frequency tail. The Raman band of the Lys-DLys peptide at 5% w/w also displays some degree of skewedness, which could be related to an equilibrium of soluble peptides and aggregates, but the effect is too small to estimate each fraction. For the Tyr-Phe peptide, no concentration-dependent downshift was observed. To calculate the fraction of soluble peptides in a 10% sample, the following assumptions were made:

$$I_{aggregate} = I_{10\%} - X^{*}I_{1\%} \quad (1)$$

in which X is the fraction of soluble peptides, $I_{10\%}$ and $I_{1\%}$ are the Raman bands for 10 and 1% samples, normalized by integrating the surface area under the peaks, and $I_{aggregate}$ would be theoretical Raman band spectrum of a sample with pure aggregates. Assuming that this Raman band will be symmetrical, this gives the boundary condition

$$\nu_{max} - \nu_{0.5,left} = \nu_{0.5,right} - \nu_{max} \quad (2)$$

in which ν_{max} is the frequency of the aggregate peak maximum, $\nu_{0.5,left}$ is the frequency at half-maximum left of ν_{max} and $\nu_{0.5,right}$ is the frequency at half-maximum right of ν_{max}. Using this boundary condition, the fraction X of soluble peptides in 10% w/w samples of lanreotide (**1**) and DTrp-DPhe (**2**) and in the 5% w/w sample of Cys-Ala (**6**) could be estimated, by calculating $I_{aggregate}$ and measuring the skewedness of the band, for various values of *X*. In a 10% w/w sample of lanreotide, the fraction *X* of soluble peptides was estimated to be [0.2], with the Raman band of pure aggregates estimated at 1380.8 cm^{-1} with a full width at half maximum (FWHM) of 6.6 cm^{-1} (compared to a soluble peptide band at 1385.3 cm^{-1} with an FWHM of 8.9 cm^{-1}). In a 10% (w/w) sample of DTrp-DPhe (**2**) *X* was estimated to be [0.15], with the Raman band of pure aggregates estimated at 1381.6 cm^{-1} and an FWHM of 8.6 cm^{-1} (compared to a soluble peptide band at 1386.4 cm^{-1} with an FWHM of 10.9 cm^{-1}). Both peptides have a narrower Raman band for aggregates compared to soluble peptides. In particular for lanreotide, the estimated fraction of soluble peptides is in agreement with the critical nanotube concentration, which is about 0.27. A 5% w/w sample of Cys-Ala X was estimated to be [0.3] with the Raman band of pure aggregates at 1383 cm^{-1} with an FWHM of 7.4 cm^{-1} (compared to a soluble peptide band at 1384.5 cm^{-1} with an FWHM of 7.5 cm^{-1}).

Concerning the Tyr-Phe derivative (**5**), the insensitivity of the naphthalene Raman band with concentration reflects the incapacity for interaction. Indeed, the Tyr derivative does not self-assemble at least in the concentration range studied here [24]. The Lys-DLys derivative (**7**) self-assembles into characteristic amyloid fibers [24] and the relative small dependance of the napthalene Raman band on the peptide concentration reflects a completely different way of interaction of the naphthalene rings in the self-assembly of these peptides.

Tyrosine. Figure 4 shows the part of the Raman spectra that contains the tyrosine Fermi doublet frequencies. The Fermi doublet results from Fermi resonance between the ring-breathing vibration and the overtone of an out-of-plane bending vibration of the phenol ring (Siamwiza *et al.* [38]). The tyrosine Fermi doublet has two peaks at 850 and 830 cm^{-1} of which the

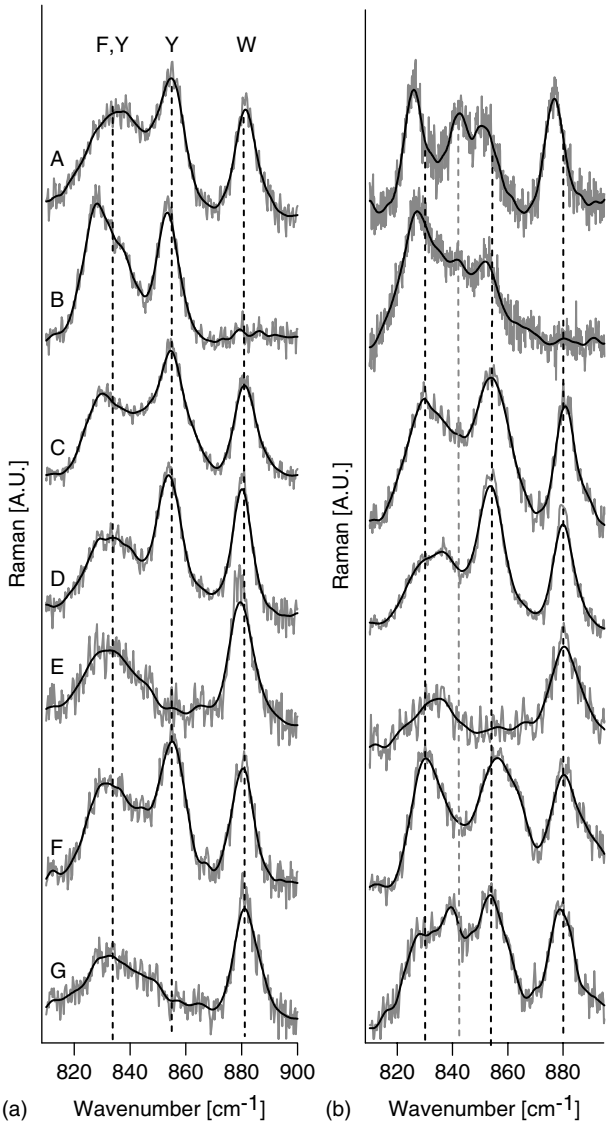

Figure 4 Raman spectra of: (A) **1** lanreotide (B) **2** DTrp-DPhe, (C) **3** DNaph-DPhe, (D) **4** DNaph-DAla, (E) **5** Tyr-Phe, (F) **6** Cys-Ala and (G) **7** Lys-DLys. (a) concentrations 1% w/w. (b): concentrations 10% w/w (A–E) or 5% w/w (F, G).

DOI: 10.1002/psc

intensity ratio I_{850}/I_{830} depends on the hydrogen-bonding state of the phenol OH-group. According to Siamwiza *et al.*, $I_{850}/I_{830} \sim 2.5$ corresponds to a strong hydrogen acceptor, $I_{850}/I_{830} \sim 1.25$ to both a hydrogen donor and acceptor and $I_{850}/I_{830} \sim 0.3$ to a strong hydrogen donor. Phenylalanine also has a band at 830 cm^{-1} that can be distinguished in Figure 4(E). Graph E shows the spectra of the Tyr-Phe peptide (**5**), in which the tyrosine is replaced by a phenylalanine. The left panel shows the spectra for soluble concentrations. Differences in the tyrosine doublet ratios represent the variation in the local environment of the tyrosines in the different peptide solutions. According to their 850/830 ratios, in peptide solutions the tyrosine of lanreotide (**1**) and Cys-Ala (**6**) acts both as a hydrogen donor and acceptor, the tyrosine of DNaph-DAla (**4**) is a strong hydrogen acceptor and the tyrosine of Lys-DLys (**7**) a strong hydrogen donor. For peptides DTrp-DPhe (**2**) and DNaph-DPhe (**3**) interpretation is hampered due to the presence of a phenylalanine band. Interestingly, at high peptide concentrations (Figure 4, b) the tyrosine doublet of lanreotide (**1**), DTrp-DPhe (**2**) and Lys-DLys (**7**) has a very unusual character, containing three distinctive bands at 825, 840 and 855 cm^{-1} respectively. Heterogeneity of the tyrosines in aggregates could cause a splitting of one of the vibrational modes, resulting in three peaks instead of a doublet. Because the referred Raman spectra are recorded from samples containing a coexistence of soluble peptides and nanostructure aggregates, the three bands could originate from heterogeneity of the mixtures. However, for lanreotide and the DTrp-DPhe samples we have an estimate of the fraction of soluble peptides in a 10% w/w sample [respectively (0.2) and (0.15)]. For lanreotide it was verified that subtraction of the estimated fraction of the soluble peptide spectrum from the spectrum of the 10% w/w/sample would leave a 'pure aggregate' spectrum containing three peaks ($I_{agg} = I_{10\%} - [0.2]^{*}I_{1\%}$ with $I_{10\%}$ the 10% w/w sample and $I_{1\%}$ the 1% w/w sample). This implies that in the lanreotide nanotubes heterogeneity occurs within the aggregates, such as a molecular packing containing two alternating tyrosine side chain conformations. Alternatively, very specific intermolecular interactions involving tyrosine could affect the doublet in a highly unusual way. Regardless of the explanation for the three bands in the doublet, similarity of the Raman bands for the three peptides strongly suggests that these peptides share a structural motif for the tyrosine phenol group in the self-assemblies. The Cys-Ala peptide (**6**) that forms curved lamellar sheets at high peptide concentrations does not show this phenomenon and only has a small change of its 850/830 ratio compared to its soluble peptide spectrum. The DNaph-DPhe peptide (**3**) shows a small increase of its 830 band at high concentration where as DNaph-DAla (**4**) does not show any change. It was found that both the naphthylalanine-modified derivatives **3** and **4** form micelle-like structures at high concentrations [24]. It is likely that the local environment of tyrosine in DNaph-DAla or phenylalanine in DNaph-DPhe changes upon micelle formation and has a small effect on its Raman frequencies.

Tryptophan. The vibrational mode νW17 around 880 cm^{-1} (Figure 4) reflects the strength of H-bonding at the N_1H side of the indole ring [39]. This mode is sensitive to the environment of the tryptophan indole –NH group and can shift from 883 cm^{-1} in a non-bonded state toward 860 cm^{-1} in case of a strongly hydrogen-bonded state. A value of 877 cm^{-1} has been reported for weak hydrogen bonding of this group to water molecules [40]. Except for lanreotide, the peptides have a Raman band at 880 cm^{-1} for both the soluble (1% w/w) and self-assembled (5 and 10% w/w) states. Lanreotide shows a downshift towards 877 cm^{-1} upon self-assembly, corresponding to a water-bound state of the indole ring.

The vibrational mode νW3 around 1550 cm^{-1} (Figure 5) arises from an indole ring vibration mainly contributed from the $C_2{=}C_3$ stretch and is sensitive to rotation of the tryptophan indole side chain around the C_β—C_3 bond (torsion angle $|\chi|^{2,\,1}$) [40]. Table 2 presents the calculated torsion angles for the peptide solutions and nanostructure self-assemblies. Upon self-assembly, lanreotide, Cys-Ala and Lys-DLys (**1, 6** and **7**) show a 5–12° change in the orientation of $|\chi|^{2,\,1}$. For lanreotide self-assembly, we have shown that the mutation of Trp into Phe only changes the final monodisperse diameter of the nanotubes [22]. This observation leads to the conclusion that the aromatic that is controlling the diameter should be in close contact between protofilaments and therefore self-assembly should lead to a change in the orientation of the aromatic side chain. In the case of Cys-Ala and Lys-DLys, the Raman spectra also show a change of the orientation of the indole upon self-assembly, suggesting a possible role of the Trp in the other types of self-assemblies, i.e. lamellae for Cys-Ala and amyloid fibers for Lys-DLys.

Structural Motifs for Self-Assembly into Nanotubes, Fibers or Lamellar Sheets

Both lanreotide and DTrp-DPhe (**2**) form nanotubes with a high degree of ordering that are exceptionally long. The nanotube assemblies are characterized by down-shifted naphthalene Raman frequencies, by a highly unusual Raman feature for the tyrosine doublet and for lanreotide also by an unusual low tryptophan fluorescence polarization. According to their behavior all three aromatic residues are involved in intermolecular packing interactions. In the supramolecular packing for lanreotide and DTrp-DPhe, the double-layered nanotube walls are built up from two types of filaments, formed

DOI: 10.1002/psc

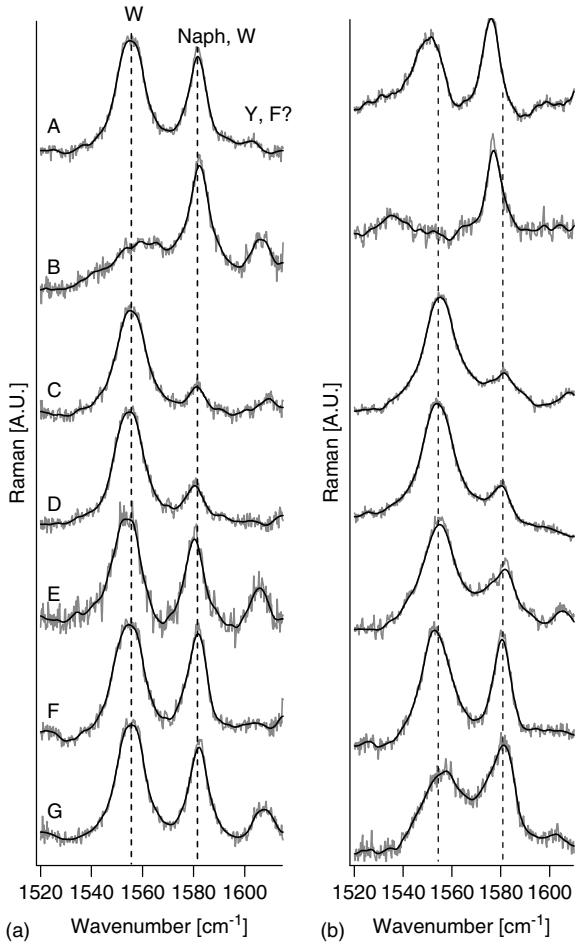

Figure 5 Raman spectra of: (A) **1** lanreotide (B) **2** DTrp-DPhe, (C) **3** DNaph-DPhe, (D) **4** DNaph-DAla, (E) **5** Tyr-Phe, (F) **6** Cys-Ala and (G) **7** Lys-DLys. (a) concentrations 1% w/w. (b) concentrations 10% w/w (A–E) or 5% w/w (F, G).

Table 2 Calculated dihedral angles of soluble peptides and nanostructure assemblies[a]

Peptide	Soluble νW3 [cm^{-1}]	Soluble $\lvert\chi\rvert^{2,1}$	Aggregate νW3 [cm^{-1}]	Aggregate $\lvert\chi\rvert^{2,1}$
1 (lanreotide)	1555.5	108°	1551.0	95°
6 (Cys-Ala derivative)	1555.0	106°	1553.5	101°
7 (Lys-DLys derivative)	1556.0	110°	1557.5°	122°

[a] For the soluble samples the peptide concentration was 1% w/w and for the aggregate samples the peptide concentrations were 5% w/w (Cys-Ala and Lys-DLys) or 10% w/w (lanreotide). The dihedral angles were calculated using the following formula [40]: $\nu = 1542 + 6.7^{*}[\cos 3|\chi|^{2,1} + 1]^{1.2}$

by antiparallel stacked peptides (illustrated in Figure 1 (b)). Within the filaments Tyr-Tyr and Thr-Val intermolecular interactions (type 1 filament) and Nal-Tyr and Val–Val intermolecular interactions (type 2 filament) could occur. Between the filaments, Tyr-Tyr and Tyr-Naph interactions could occur. The model does not give information on the lateral association of filaments to form tubes. However, the fact that the DTrp => DPhe modification reduces the tube diameter from 24to 18 nm suggests that the aromatic residue at the 4th position is involved in the lateral interaction between the filaments. The importance of the naphthalene group is illustrated by the fact that the naphthalene-modified peptides DNaph-DPhe and DNaph-DAla (**3** and **4**) are incapable of self-assembly into ordered nanostructures. Here we observe a downshift for the naphthalene frequency modes in the nanotube assemblies and conclude from a test experiment on naphthalene in various solvents that this downshift is not caused by a change in polarity of the environment. At this point we have no clear explanation for the observed downshift, but it might be connected to molecular interactions that influence the ring flatness or breathing modes. Narrowing of the Raman bands reveals a more homogeneous distribution upon self-assembly that could originate from restricted mobility of the naphthalene side chains inside the nanotubes. The similar shift for the lanreotide (**1**) and DTrp-DPhe (**2**) nanotube assemblies, compared to the smaller downshift observed for the Cys-Ala (**6**) and Lys-DLys (**7**) resp. sheet and fiber assemblies, suggests a correlation with the specific molecular packing of the naphthalene rings in the assemblies.

The Raman and fluorescence data suggest that in all the assemblies the tryptophan residues reside in a hydrophilic environment, in which the indole NH is capable of hydrogen bonding to water molecules. The position of the W17 band around 877–880 cm^{-1} makes it unlikely that the indole NH-group is involved in a strong intermolecular hydrogen bond. The results imply that the Trp sidechains are not fully embedded in the walls of the nanostructures, i.e. pointing inwards and outwards to the water environment or surrounded by surface-bound water molecules. 1H NMR spectra of lanreotide solutions show upfield ring current shifts of the Trp C_γ peaks due to Trp-Lys interactions in the turn of the hairpin [41]. In lanreotide nanotubes, the lysine side chain may have a stabilizing role through repetitive lateral interfilament Trp-Lys interactions: the lysine sidechains are positively charged and thus are also expected to be oriented towards the water environment. In addition, the low fluorescence polarization and change in torsion angle compared to the soluble peptides reveal that the indole groups are involved in aromatic packing interactions. A most likely explanation for the low polarization value is the occurrence of Trp-Trp fluorescence energy transfer. Trp-Trp stacking could be a stabilizing motif in both nanotube (lanreotide) and fiber (Lys-DLys (7)) assemblies. For lanreotide nanotubes this implies that Trp-Trp interactions modulate the curvature of the

DOI: 10.1002/psc

nanotubes. The importance of the tyrosine residue in the self-assembly of lanreotide has been demonstrated by the fact that no ordered structures are formed by the Tyr-Phe peptides (**5**). Notably, the loss of the ordered structures upon replacement of Tyr by Phe has shown that specific aromatic interactions or the hydrogen bonding capacity of the phenoxyl OH-group account for the stability of the self-assemblies. The Raman spectra of lanreotide (**1**), DTrp-DPhe (**2**) and the Lys-DLys (**7**) peptides show a remarkable effect of three bands appearing in the Tyr Fermi doublet upon self-assembly. So far, the most unusual Raman signature that has been reported was a singlet ~854 cm^{-1} which has been attributed to a nonhydrogen-bonded state of the tyrosine phenoxyl group [42]. The molecular and supramolecular packing for lanreotide and DTrp-DPhe (**2**) nanotubes assumes that the Tyr side chains are involved in several intermolecular interactions that stabilize the filament β-sheets and the double layer formed by the two types of filaments. Splitting of the Tyr doublet into three bands could therefore originate from heterogeneity, assuming two different orientations of Tyr in the assemblies. It is interesting that the Lys-DLys (**7**) assemblies share the unusual Raman signature for the tyrosine Fermi doublet. It is expected that the change in the isomerization of the lysine residue changes the repartition of the hydrophobic groups in relation to the peptide backbone, resulting in different molecular packing in the fiber filaments. However, the tyrosine Fermi doublet Raman feature suggests a common role for the tyrosine residue to stabilize fiber and nanotube assemblies. The Cys-Ala (**6**) lamellar sheet assemblies lack the splitting of the tyrosine Fermi doublet into three bands and do not show a large downshift of the naphthalene Raman freqencies. The combined results suggest that deletion of the disulfide bridge leads to different nanostructures (i.e. sheets instead of tubes) that are stabilized by different intermolecular interactions compared to the ones stabilizing lanreotide nanotubes.

CONCLUSIONS

Aromatic interactions play a key role in the formation of various types of amyloid fibers, underlining the general importance for elucidating shared motifs and spectroscopic characteristics of peptide β-sheet assemblies. A combination of fluorescence and Raman spectroscopy allowed us to probe the environment of the aromatic residues of a set of synthetic octapeptides, comparing nonassembled to the self-assembled peptides. For the two peptides that form nanotubes, results are in agreement with a molecular and supramolecular packing in which the nanotubes are stabilized by (1) naphthalene side chains, which might be involved in specific molecular interactions or orientations, (2) tyrosines that stabilize the filaments and the double-walled layer of filaments and (3) Trp–Trp aromatic packing, in which the tryptophans are oriented inward or outward from the nanotube layers towards the water environment and which modulate the curvature of the tubes. The fiber assemblies formed by the Lys-DLys peptides that have a less-structured hairpin conformation also appear to involve intermolecular Trp–Trp and tyrosine interactions. Self-assemblies of this peptide share an unusual Raman signature for tyrosine with the nanotube assemblies, suggesting a common role for tyrosine to stabilize antiparallel β-sheet filaments in fibers and nanotubes. Estimations of the tryptophan dihedral angles in the soluble peptides and nanostructures can be used as conformational constraints for further structural analysis. The lamellar sheet assemblies formed by the cysteine-bearing peptides lack the tyrosine and naphthalene Raman characteristics. This indicates that transformation of the cyclic peptide lanreotide into a linear peptide results in self-assemblies that are stabilized by different molecular/aromatic interactions compared to lanreotide ones.

Supplementary Material

Supplementary electronic material for this paper is available in Wiley InterScience at: http://www.interscience.wiley.com/jpages/1075-2617/suppmat/

Acknowledgements

A.P. is grateful to the Netherlands Organization of Scientific Research (NWO) for granting a Talent grant and to Ipsen/Pharma for financial support through an industrial contract between Ipsen/Pharma and the Peptide Self-Assembly group, iBiTechS, Cea. This work has also been partially funded by the ANR-RIB, THERA-PEP. Dr Jean-Christophe Cintrat is greatly acknowledged for drying the organic solvents used to study the effect of solvent polarity on the FT-Raman spectrum of naphthalene.

REFERENCES

1. Zhang SG. Fabrication of novel biomaterials through molecular self-assembly. *Nat. Biotechnol.* 2003; **21**(10): 1171–1178.
2. Sarikaya M, Tamerler C, Jen AKY, Schulten K, Baneyx F. Molecular biomimetics: nanotechnology through biology. *Nat. Mater.* 2003; **2**(9): 577–585.
3. Turro JN. Molecular structure as a blueprint for supramolecular structure chemistry in confined spaces. *Proc. Natl. Acad. Sci. U.S.A.* 2005; **102**: 10 766–10 770.
4. Lehn JM. *Supramolecular Chemistry*. John Wiley: New York, 1995.
5. Dobson CM. Protein folding and misfolding. *Nature* 2003; **426**(6968): 884–890.
6. Makin OS, Atkins E, Sikorski P, Johansson J, Serpell LC. Molecular basis for amyloid fibril formation and stability. *Proc. Natl. Acad. Sci. U.S.A.* 2005; **102**(2): 315–320.
7. Perutz MF, Finch JT, Berriman J, Lesk A. Amyloid fibers are water-filled nanotubes. *Proc. Natl. Acad. Sci. U.S.A.* 2002; **99**(8): 5591–5595.

8. Jimenez JL, Guijarro JL, Orlova E, Zurdo J, Dobson CM, Sunde M, Saibil HR. Cryo-electron microscopy structure of an SH3 amyloid fibril and model of the molecular packing. *EMBO J.* 1999; **18**(4): 815–821.
9. Plakoutsi G, Bemporad F, Calamai M, Taddei N, Dobson CM, Chiti F. Evidence for a mechanism of amyloid formation involving molecular reorganisation within native-like precursor aggregates. *J. Mol. Biol.* 2005; **351**: 910–922.
10. Sasahara K, Naiki H, Goto Y. Kinetically controlled thermal response of β2-microglobulin amyloid fibrils. *J. Mol. Biol.* 2005; **352**: 700–711.
11. Shivaprasad S, Wetzel R. An intersheet packing interaction in A beta fibrils mapped by disulfide cross-linking. *Biochemistry* 2004; **43**(49): 15 310–15 317.
12. Sabate R, Estelrich J. Evidence of the existence of micelles in the fibrillogenesis of beta-amyloid peptide. *J. Phys. Chem. B* 2005; **109**(21): 11 027–11 032.
13. Caplan MR, Moore PN, Zhang SG, Kamm RD, Lauffenburger DA. Self-assembly of a beta-sheet protein governed by relief of electrostatic repulsion relative to van der Waals attraction. *Biomacromolecules* 2000; **1**(4): 627–631.
14. Porat Y, Mazor Y, Efrat S, Gazit E. Inhibition of islet amyloid polypeptide fibril formation: A potential role for heteroaromatic interactions. *Biochemistry* 2004; **43**(45): 14 454–14 462.
15. de la Paz ML, Goldie K, Zurdo J, Lacroix E, Dobson CM, Hoenger A, Serrano L. De novo designed peptide-based amyloid fibrils. *Proc. Natl. Acad. Sci. U.S.A.* 2002; **99**(25): 16 052–16 057.
16. Hosia W, Bark N, Liepinsh E, Tjernberg A, Persson B, Hallen D, Thyberg J, Johansson J, Tjernberg L. Folding into a beta-hairpin can prevent amyloid fibril formation. *Biochemistry* 2004; **43**(16): 4655–4661.
17. Zhang SG, Marini DM, Hwang W, Santoso S. Design of nanostructured biological materials through self-assembly of peptides and proteins. *Curr. Opin. Chem. Biol.* 2002; **6**(6): 865–871.
18. Ghadiri MR, Granja JR, Milligan RA, McRee DE, Khazanovich N. Self-assembling organic nanotubes based on a cyclic peptide architecture. *Nature* 1993; **366**(6453): 324–327.
19. Reches M, Gazit E. Casting metal nanowires within discrete self-assembled peptide nanotubes. *Science* 2003; **300**(5619): 625–627.
20. Behanna HA, Donners J, Gordon AC, Stupp SI. Coassembly of amphiphiles with opposite peptide polarities into nanofibers. *J. Am. Chem. Soc.* 2005; **127**(4): 1193–1200.
21. Nowak AP, Breedveld V, Pakstis L, Ozbas B, Pine DJ, Pochan D, Deming TJ. Rapidly recovering hydrogel scaffolds from self-assembling diblock copolypeptide amphiphiles. *Nature* 2002; **417**(6887): 424–428.
22. Valéry C, Paternostre M, Robert B, Gulik-Krzywicki T, Narayanan T, Dedieu JC, Keller G, Torres ML, Cherif-Cheikh R, Calvo P, Artzner F. Biomimetic organization: octapeptide self-assembly into nanotubes of viral capsid-like dimension. *Proc. Natl. Acad. Sci. U.S.A.* 2003; **100**(18): 10 258–10 262.
23. Valéry C, Artzner F, Robert B, Gulick T, Keller G, Grabielle-Madelmont C, Torres ML, Cherif-Cheikh R, Paternostre M. Self-association process of a peptide in solution: from beta-sheet filaments to large embedded nanotubes. *Biophys. J.* 2004; **86**(4): 2484–2501.
24. Valéry C, Pouget E, Pandit A, Verbavatz J-M, Bordes L, Boisdé I, Cherif-Cheikh R, Artzner F, Paternostre M. Molecular origin of the self-assembly of lanreotide into nanotubes- a mutational approach, *Biophys. J.* (in press).
25. Virshow R. Ueber eine im Gehim und Rückenmark des Menschen aufgefundene Substanz mit der chemischen reaction der cellulose. *Virshow Arch. Pathol. Anat. Physiol.* 1854; **6**: 135–138.
26. Divry P, Flokin M. les propriétés optiques des amyloides. *C. R. Soc. Biol. (Paris)* 1927; **97**: 1808–1810.
27. Levine H. Thioflavine-T Interaction with synthetic Alzheimers-disease beta-amyloid peptides – detection of amyloid aggregation in solution. *Protein Sci.* 1993; **2**(3): 404–410.
28. Petkova AT, Leapman RD, Guo ZH, Yau WM, Mattson MP, Tycko R. Self-propagating, molecular-level polymorphism in Alzheimer's beta-amyloid fibrils. *Science* 2005; **307**(5707): 262–265.
29. Kowalewski T, Holtzman DM. In situ atomic force microscopy study of Alzheimer's beta-amyloid peptide on different substrates: new insights into mechanism of beta-sheet formation. *Proc. Natl. Acad. Sci. U.S.A.* 1999; **96**(7): 3688–3693.
30. Arimon M, Diez-Perez I, Kogan MJ, Durany N, Giralt E, Sanz F, Fernandez-Busquets X. Fine structure study of A beta(1–42) fibrillogenesis with atomic force microscopy. *FASEB J.* 2005; **19**(7): 1344–1346.
31. Krebs MRH, Bromley EHC, Donald AM. The binding of thioflavin-T to amyloid fibrils: localisation and implications. *J. Struct. Biol.* 2005; **149**(1): 30–37.
32. Lorenzo A, Yankner BA. Beta-amyloid neurotoxicity requires fibril formation and is inhibited by congo red. *Proc. Natl. Acad. Sci. U.S.A.* 1994; **91**(25): 12 243–12 247.
33. Mattioli TA, Williams JC, Allen JP, Robert B. Changes in primary donor hydrogen-bonding interactions in mutant reaction centers from Rhodobacter-Sphaeroides – identification of the vibrational frequencies of all the conjugated carbonyl groups. *Biochemistry* 1994; **33**(7): 1636–1643.
34. Larsen OFA, van Stokkum IHM, Pandit A, van Grondelle R, van Amerongen H. Ultrafast polarized fluorescence measurements on tryptophan and a tryptophan-containing peptide. *J. Phys. Chem. B* 2003; **107**(13): 3080–3085.
35. Pandit A, Larsen OFA, van Stokkum IHM, van Grondelle R, Kraayenhof R, van Amerongen H. Ultrafast polarized fluorescence measurements on monomeric and self-associated melittin. *J. Phys. Chem. B* 2003; **107**(13): 3086–3090.
36. Moens PDJ, Helms MK, Jameson DM. Detection of tryptophan to tryptophan energy transfer in proteins. *Protein J.* 2004; **23**(1): 79–83.
37. Kayser V, Turton DA, Aggeli A, Beevers A, Reid GD, Beddard GS. Energy migration in novel pH-Triggered self-assembled beta-sheet ribbons. *J. Am. Chem. Soc.* 2004; **126**(1): 336–343.
38. Siamwiza MN, Lord RC, Chen MC, Takamatsu T, Harada I, Matsuura H, Shimanouchi T. Interpretation of doublet at 850 and 830 Cm^{-1} in Raman-spectra of tyrosyl residues in proteins and certain model compounds. *Biochemistry* 1975; **14**(22): 4870–4876.
39. Miura T, Takeuchi H, Harada I. Characterization of individual tryptophan side-chains in proteins using Raman-spectroscopy and hydrogen-deuterium exchange kinetics. *Biochemistry* 1988; **27**(1): 88–94.
40. Takeuchi H. Raman structural markers of tryptophan and histidine side chains in proteins. *Biopolymers* 2003; **72**(5): 305–317.
41. Verheyden PMF, Coy DH, Vanbinst G. Conformational study of somatostatin analogs in methanol at low-temperature. *Magn. Reson. Chem.* 1991; **29**(6): 607–612.
42. Arp Z, Autrey D, Laane J, Overman SA, Thomas GJ. Structural studies of viruses by Raman spectroscopy part LXXI – Tyrosine Raman signatures of the filamentous virus Ff are diagnostic of non-hydrogen-bonded phenoxyls: demonstration by Raman and infrared spectroscopy of p-cresol vapor. *Biochemistry* 2001; **40**(8): 2522–2529.